Wang *et al. Microstructures* **2025**, *5*, 2025097
DOI: 10.20517/microstructures.2025.31

Microstructures

Research Article

Open Access

Check for updates

Achieving near-zero thermal expansion over a wide temperature range in $(Hf,Ta)(Fe,Cr)_2$ alloys

Xiaobo Wang[1,#], Minjun Ai[1,#], Feixiang Long[1], Hong Zhong[1], Hao Lu[1], Chang Zhou[1,2], Jun Chen[1]

[1]Beijing Advanced Innovation Center for Materials Genome Engineering, Department of Physical Chemistry, University of Science and Technology Beijing, Beijing 100083, China.
[2]State Key Laboratory for Advanced Metals and Materials, University of Science and Technology Beijing, Beijing 100083, China.
[#]These authors contributed equally to this work.

Correspondence to: Assoc. Prof. Chang Zhou, State Key Laboratory for Advanced Metals and Materials, University of Science and Technology Beijing, Beijing 100083, China. E-mail: changzhou@ustb.edu.cn

How to cite this article: Wang, X.; Ai, M.; Long, F.; Zhong, H.; Lu, H.; Zhou, C.; Chen, J. Achieving near-zero thermal expansion over a wide temperature range in $(Hf,Ta)(Fe,Cr)_2$ alloys. *Microstructures* **2025**, *5*, 2025097. https://dx.doi.org/10.20517/microstructures.2025.31

Received: 12 Mar 2025 **First Decision:** 14 May 2025 **Revised:** 18 May 2025 **Accepted:** 26 May 2025 **Published:** 28 Oct 2025

Academic Editor: Andrea Sanson **Copy Editor:** Ting-Ting Hu **Production Editor:** Ting-Ting Hu

Abstract

Zero thermal expansion alloys possess significant potential for applications in aerospace, electronics, and optical instruments because their volume remains nearly constant despite temperature changes. Regulating and exploring zero thermal expansion alloys is crucial to mitigating thermal strain and stress. This study successfully adjusted negative thermal expansion alloy (Hf, Ta)Fe_2 to zero thermal expansion over a wide temperature range by optimizing its composition and controlling the magnetic phase transition. Moderately substituting Cr for Fe transformed the giant negative thermal expansion (ΔT = 15 K) into near-zero thermal expansion (ΔT = 200 K). High-resolution synchrotron X-ray diffraction, macroscopic magnetic measurements, and linear thermal expansion measurements were employed to investigate the crystalline structures, magnetic properties, and thermal expansion of $Hf_{0.84}Ta_{0.16}Fe_{2-x}Cr_x$ ($0 \le x \le 0.25$). The alignment of the magnetic phase transition and anomalous thermal expansion temperature ranges demonstrates the essential role of spin-lattice coupling. This work offers valuable insights into regulating zero thermal expansion behavior and explaining the applications of magnetic negative thermal expansion alloys. This advancement will promote their use in high-precision instruments, aerospace, microelectronics, and advanced manufacturing, enhancing device reliability and performance, particularly in extreme temperature environments.

Keywords: Near-zero thermal expansion, magnetic phase transition, negative thermal expansion, kagome structure

© The Author(s) 2025. **Open Access** This article is licensed under a Creative Commons Attribution 4.0 International License (https://creativecommons.org/licenses/by/4.0/), which permits unrestricted use, sharing, adaptation, distribution and reproduction in any medium or format, for any purpose, even commercially, as long as you give appropriate credit to the original author(s) and the source, provide a link to the Creative Commons license, and indicate if changes were made.

INTRODUCTION

Zero thermal expansion (ZTE) is a rare and precious property where the material exhibits negligible volume change with increasing temperature[1,2]. ZTE occurs when the contraction of at least one dimension of the material with rising temperature compensates for the positive thermal expansion (PTE), resulting in negligible volume change[3,4]. This anomalous behavior has attracted considerable research interest, providing a basis for understanding the physical nature of thermal expansion, and leading to the development of a new class of functional materials with unique practical value[5,6]. Research on anomalous thermal expansion dates back to 1897, when Guillaume first discovered ZTE in Invar alloys[7]. This alloy series, along with the later discovered magnetic negative thermal expansion (NTE) alloys, has been essential in aerospace remote sensors, high-pressure compressor casings, frequency generators, and printed circuit boards, due to their ability to compensate for PTE and their excellent thermal conductivity[8,9,10]. Magnetic NTE alloys can also be tuned into ZTE alloys directly. Developing high-performance ZTE alloys requires significant effort, and their practicality is often limited by narrow working temperature ranges[11,12]. Thus, regulating the magnetism and temperature range of NTE alloys is crucial for enhancing their versatility and applicability, maximizing their potential in various technological applications[13,14].

The NTE property of solid materials is due to the synergy of lattice vibration, electron transition, and phonon interaction[15]. When the NTE behavior generated by mechanisms such as anharmonic vibration, magnetic moment rearrangement, or charge transfer exceeds the PTE behavior of the lattice, the material presents a phenomenon of macroscopic volume contraction. According to the different action mechanisms, NTE materials can be divided into phonon-driven and electron-driven types. Phonon-driven NTE compounds are mainly based on an open framework structure (such as ZrW_2O_8)[16], and this type of NTE material achieves lattice contraction through the transverse vibration of bridge oxygen atoms or the coupling rotation of polyhedra. The electron-transition-induced type includes mechanisms such as magnetism (the magnetovolume effect of $Fe_{65}Ni_{35}$ Invar alloy), ferroelectricity (such as the ferroelectric-paraelectric phase transition of $PbTiO_3$)[17], and charge transfer (such as the charge rearrangement of $BiNiO_3$)[18]. The electron-transition-induced NTE materials mainly regulate the lattice volume through changes in the electronic state, among which magnetic NTE has become a hot research direction in the electron-transition type due to its unique magneto-lattice coupling characteristics[19].

Chemical substitution is one of the most effective methods for regulating thermal expansion in NTE materials. It affects thermal expansion by introducing defects and stress, and altering the material's magnetism[20]. For instance, Song *et al.* achieved ZTE in $TbCo_2$ by substituting Fe in the Co sublattice[21]. Similarly, Huang *et al.* incorporated Co into $La(Fe, Si)_{13}$ to expand its NTE temperature range and broaden the temperature window in $La(Fe, Co, Si)_{13}$[22]. Additionally, Li *et al.* employed the method of interstitial atom doping. They achieved ZTE in $La(Fe, Si)_{13}$ by doping hydrogen atoms into the lattice[23]. Xu *et al.* regulated $HfFe_2$ by changing the non-stoichiometric ratio and successfully broadened its NTE temperature window[24]. In addition to these traditional methods, some novel approaches have also been put forward. For instance, Yuan *et al.* broadened the NTE temperature range of Mn_3GaN by increasing the configurational entropy of Ga-site[25]. Xu *et al.* modulated the thermal expansion coefficient of PTE $HfFe_2$ to $1.25 \times 10^{-6} \cdot K^{-1}$ in the temperature range of 433-583 K through non-stoichiometric engineering. Regulating PTE to ZTE or NTE is highly meaningful, and various attempts have been made to realize ZTE or NTE in the $HfFe_2$ series[24]. Cen *et al.* substituted Ta into the structure and obtained (Hf, Ta)Fe_2 with NTE performance. When the temperature is between 222-327 K, the thermal expansion coefficient reaches $-16.3 \times 10^{-6} \cdot K^{-1}$, making it a very promising NTE material[26]. However, the large NTE of (Hf, Ta)Fe_2 caused by a first-order magnetic phase transition is difficult to regulate to ZTE, especially due to the narrow and low temperature range. Therefore, the regulation of thermal expansion of (Hf, Ta)Fe_2 has become a focus of research aiming to fully exploit its application potential[27,28,29].

Herein, ZTE in $Hf_{0.84}Ta_{0.16}Fe_{1.9}Cr_{0.1}$ at room temperature was achieved by moderately substituting Fe with Cr. We successfully broadened the temperature range to 165-365 K with a CTE of $1.55 \times 10^{-6}\cdot K^{-1}$. By refining the synchrotron X-ray diffraction (SXRD) profiles and analyzing the magnetic data and the thermal expansion data, it can be concluded that the thermal expansion of (Hf, Ta) Fe_2 is mainly determined by the magnetoelastic coupling effect of Fe(6h). Cr substitution alters the Fe-Fe pair spacing, weakening the magnetic interaction and reducing the interaction between iron atoms[30]. The reduced interaction between iron atoms weakens the NTE trend, and the slowdown in this process results in the emergence of ZTE. This is beneficial for broadening the NTE temperature window of (Hf, Ta)Fe_2.

EXPERIMENTAL

A series of $Hf_{0.84}Ta_{0.16}Fe_{2-x}Cr_x$ ($0 \le x \le 0.25$) samples were all melted in an arc furnace under a high-purity argon atmosphere. The raw materials were all high-purity metals of Hf, Ta, Fe, and Cr, with a purity of 99.99%. To ensure the uniformity of the ingots, the melting operation was repeated 4-5 times for each ingot. During each melting process, the ingot was turned over. After the melting process was completed, the ingot was wrapped with molybdenum foil and sealed in a vacuum-tight quartz tube, and then annealed in a muffle furnace at 1,223 K for 5 days before being slowly cooled down to room temperature. In addition, high-resolution SXRD patterns were collected on the BL02B2 beamline at SPring-8. The phase composition and crystal structure were analyzed, and the X-ray diffraction (XRD) patterns were refined using the program Fullprof. All the thermal expansion data of the samples were obtained using a NETZSCH thermomechanical analyzer with a heating rate of 5 K/min. To better analyze the regulation mechanisms, the macroscopic magnetic properties of the samples were measured using the Quantum Design Physical Property Measurement System (PPMS) and the Vibrating Sample Magnetometer (VSM).

RESULTS AND DISCUSSION

The XRD patterns of $Hf_{0.84}Ta_{0.16}Fe_{2-x}Cr_x$ ($0 \le x \le 0.25$) are shown in Figure 1A. The temperature-dependent XRD data for $Hf_{0.84}Ta_{0.16}Fe_2$ were collected and refined using the Rietveld method [Figure 1B]. In this study, based on the diffraction XRD data obtained under the condition of room temperature (300 K) and the corresponding refined results of $Hf_{0.84}Ta_{0.16}Fe_2$, we thoroughly analyzed its crystal structure [Figure 1C]. In $Hf_{0.84}Ta_{0.16}Fe_2$, Hf atoms and Ta atoms are mixed and jointly occupy the Wyckoff site 4f with coordinates of (1/3, 2/3, z). Meanwhile, Fe atoms are distributed in two different Wyckoff sites, namely 2a (0, 0, 0) and 6h (x, $2x$, 1/4)[31]. It is particularly noteworthy that the iron atoms located at the 6h site are arranged in the ab plane to form a unique two-dimensional kagome structure, and it is reported that this structural feature is related to the regulation of NTE through magnetic phase competition[32]. To further explore the thermal expansion characteristics of the $Hf_{0.84}Ta_{0.16}Fe_{2-x}Cr_x$, we conducted systematic tests on their macroscopic linear thermal expansion [Figure 1D]. The results showed that in the undoped state, $Hf_{0.84}Ta_{0.16}Fe_2$ exhibited a very significant NTE phenomenon. However, as the Cr element was gradually incorporated, an interesting phenomenon occurred: the NTE trend gradually became gentler. Correspondingly, the thermal expansion coefficient steadily increased, and the working temperature window was also broadened. It is especially worth mentioning that when the Cr content reached 0.1, the linear thermal expansion characteristics of the material exhibited an excellent performance of ZTE. At this time, for $Hf_{0.84}Ta_{0.16}Fe_{1.9}Cr_{0.1}$, the near-zero thermal expansion temperature range extended to 165-365 K, and the thermal expansion coefficient was as low as only $1.55 \times 10^{-6}\cdot K^{-1}$. The previously reported $Hf_{0.85}Ta_{0.15}Fe_2C_{0.01}$ by Xu *et al.* also exhibits the ZTE phenomenon with a thermal expansion coefficient of $2.4 \times 10^{-6}\cdot K^{-1}$ and an operating temperature range of 85-245 K[33]. Moreover, Xu *et al.* also regulated $HfFe_{2+\delta}$ through the non-stoichiometric methodology to achieve a thermal expansion coefficient of $1.25 \times 10^{-6}\cdot K^{-1}$ and an operating temperature range of 433-583 K[24]. Therefore, our remarkable thermal expansion regulation effects demonstrate great success and further exploit the potential of this material system in practical applications[34].

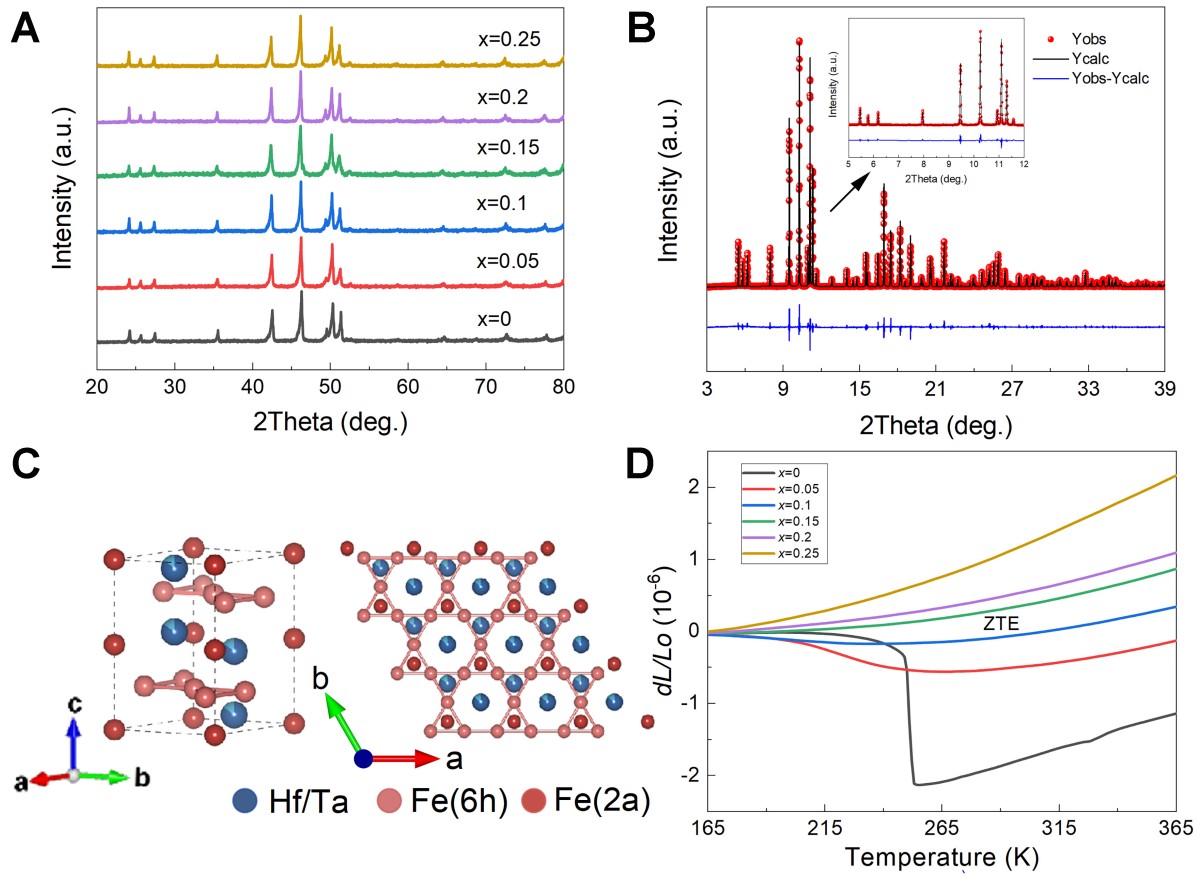

Figure 1. (A) XRD patterns of $Hf_{0.84}Ta_{0.16}Fe_{2-x}Cr_x$ ($0 \le x \le 0.25$) at room temperature; (B) Rietveld refinement plots of SXRD at room temperature for $Hf_{0.84}Ta_{0.16}Fe_2$. Red points and black lines represent observed and calculated profiles, respectively, and the difference between them is shown at the bottom of the graph; (C) Crystal structure (left) and Kagome layer on (001) plane (right) of $Hf_{0.84}Ta_{0.16}Fe_2$; (D) Linear thermal expansion ($\Delta L/L_0$) curves of $Hf_{0.84}Ta_{0.16}Fe_{2-x}Cr_x$ ($0 \le x \le 0.25$). XRD: X-ray diffraction; SXRD: synchrotron X-ray diffraction.

To clarify the changing trend of the intrinsic lattice thermal expansion, the temperature dependence of the SXRD patterns of $Hf_{0.84}Ta_{0.16}Fe_2$ within the temperature range of 100-400 K was tested [Figure 2A]. The temperature-dependent intensities of (112) and (201) peaks are specifically marked in Figure 2B. It can be roughly observed that as the temperature rises from 100 K, the diffraction peaks of (200), (112), and (201) shift toward lower angles very slowly, but when the temperature reaches 250 K, they suddenly jump to higher diffraction angles, and then shift toward lower diffraction angles as the temperature continues to increase. This directly reflects the lattice thermal expansion characteristics of $Hf_{0.84}Ta_{0.16}Fe_2$, that is, a short-lived and intense NTE at a narrow temperature range of around 250 K.

Through the structural refinement of the SXRD data, we obtained the dependence of the lattice parameters on temperature [Figure 3A]. The a-axis exhibited a relatively intense NTE phenomenon, while the c-axis showed a PTE. Since the PTE occurring on the c-axis was insufficient to exceed the intense NTE on the ab-plane, the overall volume change still demonstrated a NTE trend [Figure 3B]. This coincides with the temperature range and coefficient ratio of the macroscopic thermal expansion, thereby confirming the accuracy of the macroscopic thermal expansion measurements shown in Figure 1D.

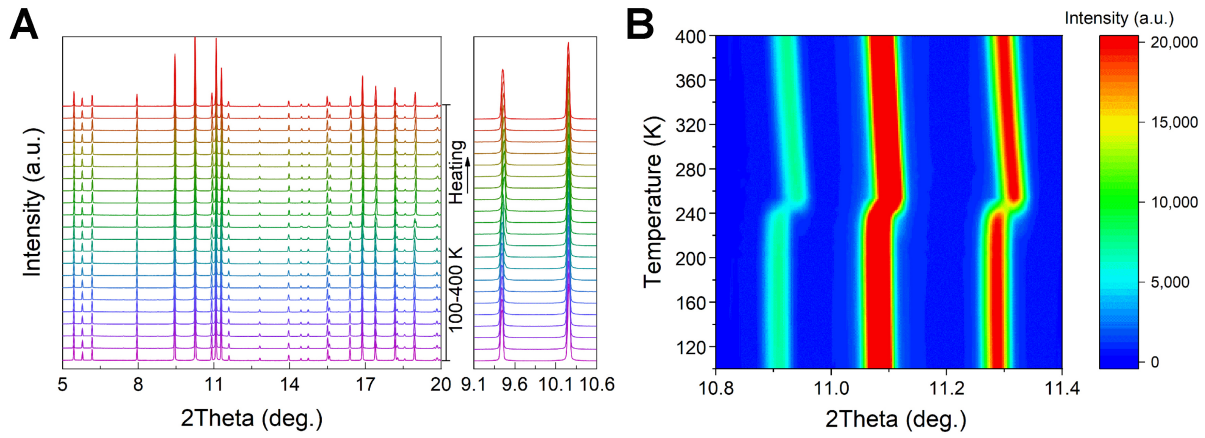

Figure 2. (A) Temperature-dependent SXRD patterns of $Hf_{0.84}Ta_{0.16}Fe_2$; (B) Temperature dependence of intensities of (200), (112), and (201) peaks in SXRD patterns. SXRD: Synchrotron X-ray diffraction.

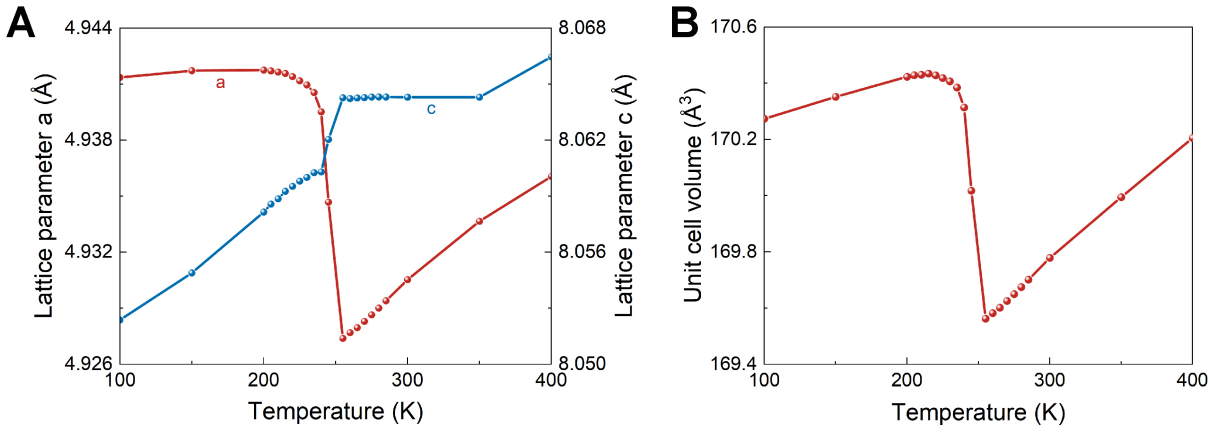

Figure 3. (A) Temperature dependence of lattice parameters a and c for $Hf_{0.84}Ta_{0.16}Fe_2$; (B) Temperature dependence of unit cell volume for $Hf_{0.84}Ta_{0.16}Fe_2$.

Furthermore, Tong has already studied that the NTE of (Hf, Ta)Fe_2 is caused by magnetic phase transitions. Using electron spin resonance (ESR) to study the magnetic phase transition, it has been confirmed that the NTE of (Hf, Ta)Fe_2 is due to spontaneous volume magnetostriction[35]. Therefore, we conducted tests on the magnetism of $Hf_{0.84}Ta_{0.16}Fe_{2-x}Cr_x$ ($0 \leq x \leq 0.25$). From the magnetic field and temperature-dependent magnetization curves, we found that $Hf_{0.84}Ta_{0.16}Fe_2$ is still ferromagnetic at low temperatures, and a phase transition to the antiferromagnetic phase occurs when the temperature rises. The addition of the Cr element makes the ferromagnetic transition more gradual. [Figure 4A]. Moreover, as the Cr content increased, the saturation magnetization of all the samples decreased accordingly [Figure 4B]. Meanwhile, we obtained T_C by measuring the extrapolated tangent line when the M-T curve undergoes a sudden change. This shows a good consistency compared with the T_C obtained from the Curie-Weiss fitting [Figure 4C]. The lower fitting data after adding Cr may be caused by the antiferromagnetism brought by Cr. We believe that in this system, the substitution of Fe atoms by Cr atoms presents a special magnetic influence mechanism. Initially, when a small number of Cr atoms entered the lattice to carry out substitution, The different electronic structures and atomic radii of Cr change the coupling interaction between magnetic atoms. With the

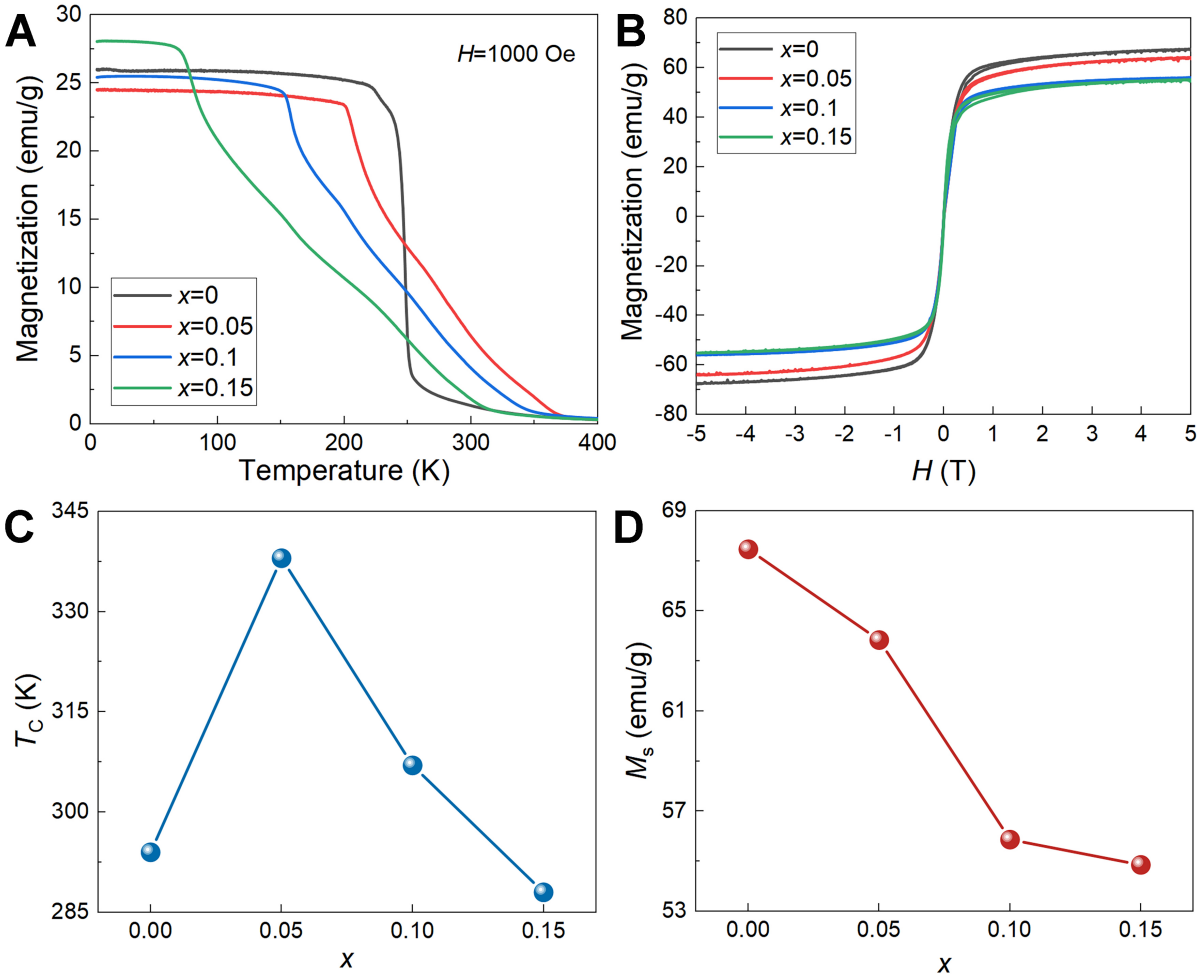

Figure 4. (A) Temperature dependence of magnetization for $Hf_{0.84}Ta_{0.16}Fe_{2-x}Cr_x$ ($0 \le x \le 0.15$); (B) Hysteresis loops of $Hf_{0.84}Ta_{0.16}Fe_{2-x}Cr_x$ ($0 \le x \le 0.15$) from -5 to 5 T at 5 K; (C) T_C and (D) M_S for $Hf_{0.84}Ta_{0.16}Fe_{2-x}Cr_x$ ($0 \le x \le 0.15$). T_C: Curie temperature; M_S: saturation magnetization.

increase of Cr content, the saturation magnetization of the compound also decreases [Figure 4D]. To some extent, this new coupling mode optimized the magnetic interactions within the system, making the cooperative arrangement of magnetic moments among atoms more orderly, thus promoting the increase in the Curie temperature (T_C). However, as the amount of Cr substitution further increased, the magnetic balance within the system was disrupted. Excessive antiferromagnetic Cr atoms led to excessive disorder in the magnetic interactions, seriously destroying the original ordered arrangement of magnetic moments, and gradually weakening the overall magnetism. Eventually, the T_C dropped to some extent. At the same time, as the chromium (Cr) content increases, the trend of the ferromagnetic transition also changes from being drastic to being more gentle. When the Cr content was 0.1, the degree of weakening of the magnetic interactions just promoted the transformation from NTE to near-zero thermal expansion.

Furthermore, since it is known that the NTE phenomenon of $Hf_{0.84}Ta_{0.16}Fe_2$ mainly occurs in the ab plane, we need to obtain the changes in the interatomic bond lengths within the ab plane for further research. Therefore, after refining the temperature-dependent XRD data, we obtained the bond lengths between Fe atoms. The bond lengths between Fe atoms at the 2a site and those at the 6h site did not show significant changes with the variation of temperature. However, interestingly, we found that the bond lengths between

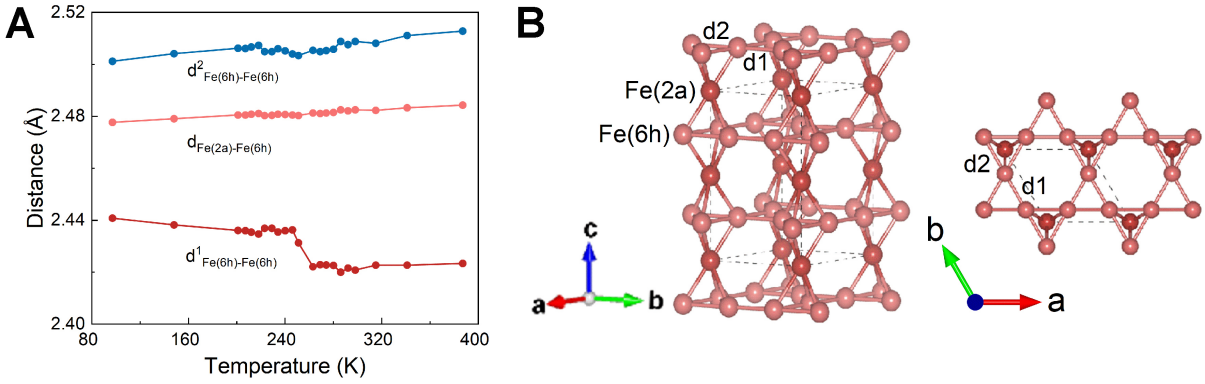

Figure 5. (A) Temperature dependence of the pair distance of different Fe - Fe pairs obtained from the refined results; (B) The position of Fe atoms and the bond lengths models of $Hf_{0.84}Ta_{0.16}Fe_2$.

Fe atoms at the 6h site within the ab plane all decreased when the temperature rose to around 250 K [Figure 5A]. Therefore, we infer that the bond length contraction between Fe atoms at the 6h position in the ab plane affects the Fe - Fe atomic interaction, which is the main reason for the NTE in $Hf_{0.84}Ta_{0.16}Fe_2$. This is also consistent with the research on the thermal expansion behavior of Kagome magnets [Figure 5B] in the ab plane of (Hf, Ta)Fe_2 conducted by Xu *et al.*[33].

To observe the relationship between magnetic changes and anomalous thermal expansion more intuitively, we fitted the thermal expansion curve with the curve of magnetic properties changing with temperature [Figure 6]. It turned out that the result was consistent with our previous speculation. For $Hf_{0.84}Ta_{0.16}Fe_2$, as the ferromagnetic phase rapidly transformed into the antiferromagnetic phase [Figure 6A], the thermal expansion curve also dropped sharply at almost the same temperature point. However, in Figure 6B, the ferromagnetic transition of $Hf_{0.84}Ta_{0.16}Fe_{1.9}Cr_{0.1}$ becomes smoother, and correspondingly, the thermal expansion curve in the same temperature range also showed a trend of becoming gentler and exhibited a near-zero thermal expansion phenomenon. This simultaneously verified the strong coupling behavior between the thermal expansion behavior and the magnetic phase transition in $Hf_{0.84}Ta_{0.16}Fe_{2-x}Cr_x$ ($0 \le x \le 0.15$)[36].

CONCLUSION

In summary, we developed a ZTE material with a thermal expansion coefficient of $1.55 \times 10^{-6}\cdot K^{-1}$ and an operating temperature range covering room temperature (165-365 K). Our strategy to regulate the NTE of $Hf_{0.84}Ta_{0.16}Fe_2$ involves chemical substitution and continuous optimization composition. The strong interaction between Fe atoms drives the NTE of $Hf_{0.84}Ta_{0.16}Fe_2$. Introducing Cr atoms weakens the magnetic interaction between Fe atoms, reducing the extent of NTE. When the Cr content reaches 0.1, the weakened and decelerated interaction between Fe atoms in the *ab* plane delays the ferromagnetic transformation, leading to ZTE. This research expands the understanding of near-zero thermal expansion regulation in (Hf, Ta)Fe_2 and highlights the potential applications of dimensionally stable materials over wide temperature ranges in advanced modern technologies[37].

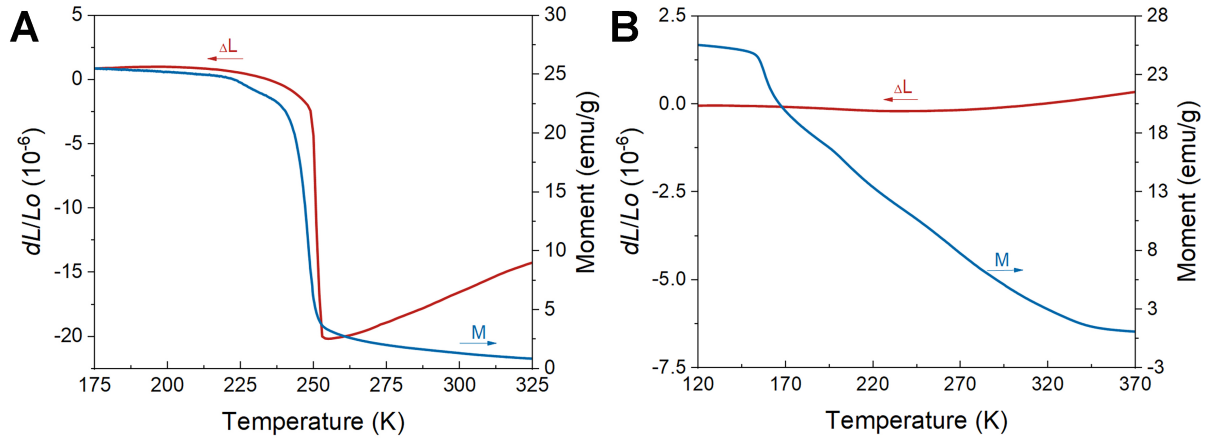

Figure 6. (A) Temperature dependence of the coefficient of thermal expansion and magnetization of $Hf_{0.84}Ta_{0.16}Fe_2$; (B) Temperature dependence of the coefficient of thermal expansion and magnetization of $Hf_{0.84}Ta_{0.16}Fe_{1.9}Cr_{0.1}$.

DECLARATIONS

Acknowledgments

The authors thank Space Environment Simulation Research Infrastructure for assistance in the experiment.

Authors' contributions

Fabricated the specimen: Wang, X.
Analyzed the diffraction data, atomic structure, and corresponding theories: Wang, X.; Ai, M.
Conceived the study and designed the research: Wang, X.
Wrote the paper: Wang, X.; Ai, M.
Contributed equally to this work: Wang, X.; Ai, M.
Read and contributed to the manuscript: Wang, X.; Ai, M.; Long, F.; Zhong, H.; Lu, H.; Zhou, C.; Chen, J.

Availability of data and materials

Data will be made available from the corresponding author upon reasonable request.

Financial support and sponsorship

This work was supported by the National Key R&D Program of China (2022YFE0109100), the Outstanding Young Scientist Program of Beijing Colleges and Universities (JWZQ20240101015), and the National Natural Science Foundation of China (22205016, 22275014, and 12104038).

Conflicts of interest

Chen, J. is the Executive Editor of the journal *Microstructures*. Chen, J. was not involved in any steps of editorial processing, notably including reviewer selection, manuscript handling, or decision making. The other authors declared that there are no conflicts of interest.

Ethical approval and consent to participate

Not applicable.

Consent for publication

Not applicable.

Copyright

© The Author(s) 2025.

REFERENCES

1. Yokoyama, T.; Eguchi, K. Anisotropic thermal expansion and cooperative Invar and anti-Invar effects in mn alloys. *Phys. Rev. Lett.* **2013**, *110*, 075901. DOI PubMed
2. Gao, Q.; Sun, Y.; Shi, N.; et al. Large isotropic negative thermal expansion in water-free Prussian blue analogues of ScCo(CN)6. *Scripta. Materialia.* **2020**, *187*, 119-24. DOI
3. Attfield, J. P. Condensed-matter physics: a fresh twist on shrinking materials. *Nature* **2011**, *480*, 465-6. DOI PubMed
4. Song, Y.; Sun, Q.; Xu, M.; et al. Negative thermal expansion in (Sc,Ti)Fe_2 induced by an unconventional magnetovolume effect. *Mater. Horiz.* **2020**, *7*, 275-81. DOI
5. Lohaus, S. H.; Heine, M.; Guzman, P.; et al. A thermodynamic explanation of the Invar effect. *Nat. Phys.* **2023**, *19*, 1642-8. DOI
6. Pang, X.; Song, Y.; Shi, N.; Xu, M.; Zhou, C.; Chen, J. Design of zero thermal expansion and high thermal conductivity in machinable xLFCS/Cu metal matrix composites. *Compos. Part. B. Eng.* **2022**, *238*, 109883. DOI
7. Schilfgaarde M, Abrikosov IA, Johansson B. Origin of the Invar effect in iron-nickel alloys. *Nature* **1999**, *400*, 46-9. DOI
8. Diop, L. V.; Amara, M.; Isnard, O. Large magnetovolume effects due to transition from the ferromagnetic to antiferromagnetic state in $Hf_{0.825}Ta_{0.175}Fe_2$ intermetallic compound. *J. Phys. Condens. Matter.* **2013**, *25*, 416007. DOI PubMed
9. Chen, F.; Xie, H.; Huo, M.; Wu, H.; Li, L.; Jiang, Z. Effects of magnetic field and hydrostatic pressure on the antiferromagnetic-ferromagnetic transition and magneto-functional properties in $Hf_{1-x}Ta_xFe_2$ alloys. *Tungsten* **2023**, *5*, 503-11. DOI
10. Dong, X.; Lin, K.; Yu, C.; et al. Zero thermal expansion in non-stoichiometric and single-phase (Hf,Nb)$Fe_{2.5}$ alloy. *Scr. Mater.* **2023**, *229*, 115388. DOI
11. Yan-jun, H.; Zhong-ying, J.; Nan, C.; Zhi-da, H.; Shu-zhen, L.; Yuan-fu, H. Magnetic properties of $Hf_{0.8}Ta_{0.2}(Fe_{0.97}A_{0.03})_2$ (A=Al, Co, Mn) systems. *Chinese. Phys. Lett.* **2006**, *23*, 3309-12. DOI
12. Duijn, H. G. M.; Brück, E.; Menovsky, A. A.; et al. Magnetic and transport properties of the itinerant electron system $Hf_{1}xTaxFe_2$. *J. Appl. Phys.* **1997**, *81*, 4218-20. DOI
13. Diop, L.; Isnard, O.; Suard, E.; Benea, D. Neutron diffraction study of the itinerant-electron metamagnetic $Hf_{0.825}Ta_{0.175}Fe_2$ compound. *Solid. State. Commun.* **2016**, *229*, 16-21. DOI
14. Ouyang, Z.; Rao, G.; Yang, H.; et al. Structure and unusual magnetic properties in the itinerant electron system $Hf_{0.8}Ta_{0.2}(Fe_{1-x}Co_x)_2$. *J. Appl. Phys.* **2004**, *370*, 18-24. DOI
15. Ma, R.; Liu, Z.; Chen, L.; et al. Transition from isotropic positive to negative thermal expansion by local Zr6O8 node distortion in MOF-801. *Microstructures* **2024**, *4*, 2024023. DOI
16. Kennedy, C. A.; White, M. A. Unusual thermal conductivity of the negative thermal expansion material, ZrW_2O_8. *Solid. State. Commun.* **2005**, *134*, 271-6. DOI
17. Jiao, Y. C.; Li, M.; Qu, B. Y.; et al. First-principles study of the negative thermal expansion of $PbTiO_3$. *Comput. Mater. Sci.* **2016**, *124*, 92-7. DOI
18. Azuma, M.; Chen, W.; Seki, H.; et al. Colossal negative thermal expansion in $BiNiO_3$ induced by intermetallic charge transfer. *Nat. Commun.* **2011**, *2*, 347. DOI PubMed PMC
19. Zheng, X. G.; Kubozono, H.; Yamada, H.; et al. Giant negative thermal expansion in magnetic nanocrystals. *Nat. Nanotechnol.* **2008**, *3*, 724-6. DOI PubMed
20. Cao, Y.; Xu, Y.; Khmelevskyi, S.; et al. Interplanar magnetic orders and symmetry-tuned zero thermal expansion in Kagomé metal (Zr,Ta)Fe_2. *Chem. Mater.* **2023**, *35*, 9167-74. DOI
21. Song, Y.; Chen, J.; Liu, X.; et al. Zero thermal expansion in magnetic and metallic Tb(Co,Fe)$_2$ intermetallic compounds. *J. Am. Chem. Soc.* **2018**, *140*, 602-5. DOI PubMed
22. Huang, R.; Liu, Y.; Fan, W.; et al. Giant negative thermal expansion in $NaZn_{13}$-type La(Fe, Si, Co)$_{13}$ compounds. *J. Am. Chem. Soc.* **2013**, *135*, 11469-72. DOI PubMed
23. Li, S.; Huang, R.; Zhao, Y.; Wang, W.; Han, Y.; Li, L. Zero thermal expansion achieved by an electrolytic hydriding method in La(Fe,Si)$_{13}$ compounds. *Adv. Funct. Mater.* **2017**, *27*, 1604195. DOI
24. Xu, M.; Song, Y.; Xu, Y.; et al. High-temperature zero thermal expansion in $HfFe_{2+\delta}$ from added ferromagnetic paths. *Chem. Mater.* **2022**, *34*, 9437-45. DOI
25. Yuan, X.; Wang, B.; Sun, Y.; et al. High□entropy anti□perovskites with enhanced negative thermal expansion behavior. *Adv. Funct. Mater.* **2024**, *34*, 2404629. DOI
26. Cen, D.; Wang, B.; Chu, R.; et al. Design of (Hf,Ta)Fe_2/Fe composite with zero thermal expansion covering room temperature. *Scr. Mater.* **2020**, *186*, 331-5. DOI
27. Bag, P.; Rawat, R.; Chaddah, P.; Babu, P. D.; Siruguri, V. Unconventional thermal effects across first-order magnetic transition in the Ta-doped $HfFe_2$ intermetallic. *Phys. Rev. B.* **2016**, *93*, 014416. DOI
28. Li, B.; Luo, X. H.; Wang, H.; et al. Colossal negative thermal expansion induced by magnetic phase competition on frustrated lattices in Laves phase compound (Hf,Ta) Fe_2. *Phys. Rev. B.* **2016**, *93*, 224405. DOI
29. Qiao, Y.; Song, Y.; Lin, K.; et al. Negative thermal expansion in (Hf,Ti)Fe_2 induced by the ferromagnetic and antiferromagnetic phase

coexistence. *Inorg. Chem.* **2019**, *58*, 5380-3. DOI PubMed

30. Wada, H.; Shimamura, N.; Shiga, M. Thermal and transport properties of $Hf_{1-x}Ta_xFe_2$. *Phys. Rev. B. Condens. Matter.* **1993**, *48*, 10221-6. DOI PubMed
31. Delyagin, N.; Erzinkyan, A.; Parfenova, V.; Rozantsev, I.; Ryasny, G. Ferromagnetic-to-antiferromagnetic transition in $(Hf_{1-x}Ti_x)Fe_2$ intermetallic compounds induced by geometrical frustration of the Fe(2a) sites. *J. Magn. Magn. Mater.* **2008**, *320*, 1853-7. DOI
32. Sun, Y.; Cao, Y.; Hu, S.; et al. Interplanar ferromagnetism enhanced ultrawide zero thermal expansion in kagome cubic intermetallic $(Zr,Nb)Fe_2$. *J. Am. Chem. Soc.* **2023**, *145*, 17096-102. DOI PubMed
33. Xu, J.; Wang, Z.; Huang, H.; et al. Significant zero thermal expansion via enhanced magnetoelastic coupling in kagome magnets. *Adv. Mater.* **2023**, *35*, e2208635. DOI PubMed
34. Diop, L. V. B.; Kastil, J.; Isnard, O.; Arnold, Z.; Kamarad, J. Collapse of ferromagnetism in itinerant-electron system: a magnetic, transport properties, and high pressure study of $(Hf,Ta)Fe_2$ compounds. *J. Appl. Phys.* **2014**, *116*, 163907. DOI
35. Li, L.; Tong, P.; Zou, Y.; et al. Good comprehensive performance of Laves phase $Hf_{1-x}Ta_xFe_2$ as negative thermal expansion materials. *Acta. Mater.* **2018**, *161*, 258-65. DOI
36. Qiao, Y.; Liaquat, I.; Zhu, Y.; Guo, J.; Liang, E.; Gao, Q. Tunable thermal expansion via the magnetic phase competition in kagome magnets. *Appl. Phys. Lett.* **2024**, *125*, 032403. DOI
37. Wang, H.; Wang, Y.; Gong, Y.; et al. Designing $(Hf,Ta)Fe_2$-based zero thermal expansion composites consisting of multiple Laves phases. *Rare. Met.* **2024**, *43*, 6596-605. DOI